Research Square

Preprints are preliminary reports that have not undergone peer review.
They should not be considered conclusive, used to inform clinical practice,
or referenced by the media as validated information.

Characterization of Allium tuberosum rottl. Peptides with Dual Inhibitory Activities against Angiotensin I Converting Enzyme and Dipeptidyl Peptidase-IV

Nhung Thi Phuong Nong
Thai Nguyen University of Agriculture And Forestry
Chia-Hui Lee
National Pingtung University of Science and Technology
Jue-Liang Hsu
jlhsu@mail.npust.edu.tw

National Pingtung University of Science and Technology https://orcid.org/0000-0002-6771-6690

Research Article

Keywords: Allium tuberosum protein, active peptides, angiotensin-I-converting enzyme, dipeptidyl peptidase-IV

Posted Date: March 20th, 2024

DOI: https://doi.org/10.21203/rs.3.rs-4080789/v1

License: This work is licensed under a Creative Commons Attribution 4.0 International License.
Read Full License

Version of Record: A version of this preprint was published at Medicinal Chemistry Research on July 25th, 2024. See the published version at https://doi.org/10.1007/s00044-024-03284-2.

Characterization of *Allium tuberosum* rottl. Peptides with Dual Inhibitory Activities against Angiotensin I Converting Enzyme and Dipeptidyl Peptidase-IV

Nhung Thi Phuong Nong[1,2#], Chia-Hui Lee[3#], and Jue-Liang Hsu[3,4,5*]

[1] Department of Basic Science, Thainguyen University of Agriculture and Forestry, Quyetthang Ward, Thai Nguyen 250000, Vietnam, nongthiphuongnhung@tuaf.edu.vn

[2]Department of Tropical Agriculture and International Cooperation, National Pingtung University of Science and Technology, Pingtung 91201, Taiwan

[3] Department of Biological Science and Technology, National Pingtung University of Science and Technology, 1 Shuefu Road, Neipu, Pingtung 91201, Taiwan, smalljia1217@gmail.com

[4] Institute of Food Safety Management, National Pingtung University of Science and Technology, Pingtung 91201, Taiwan

[5] Tropical Agriculture Research Center, National Pingtung University of Science and Technology, Pingtung, Taiwan

[#] Authors contributed equally to this work

* Corresponding author: ✉ Dr. Jue-Liang Hsu, jlhsu@mail.npust.edu.tw

ABSTRACT: Two peptides with dual functionality, namely LLPSY and NAPALVY, exhibit inhibitory effects on both angiotensin-I-converting enzyme (ACE) and dipeptidyl peptidase-IV (DPP-IV), were successfully identified from the hydrolysates of *Allium tuberosum*. Peptide isolation involved reversed-phase chromatography, and peptide sequences were characterized through liquid chromatography-tandem mass spectrometry analysis and de novo sequencing. Notably, the Lineweaver-Burk plot analysis revealed that LLPSY (IC_{50}: 15.66 ± 1.11 μM) acted in a non-competitive manner, whereas NAPALVY (IC_{50}: 3.42 ± 0.79 μM) exhibited competitive inhibition, potently inhibiting ACE. Their stability tests against ACE further revealed that LLPSY acted as a real substrate, while NAPALVY functioned as a true inhibitor of ACE. In terms of DPP-IV inhibition, LLPSY (IC_{50}: 2.48 ± 0.10 mM) was identified as a competitive inhibitor, whereas NAPALVY (IC_{50}: 7.63 ± 0.52 mM) displayed noncompetitive inhibition. Both peptides exhibited true inhibitory effects on DPP-IV. Docking simulations provided insights into peptide-enzyme interactions. These novel *Allium tuberosum*-derived peptides hold promise for controlling blood pressure and blood glucose.

Keywords: *Allium tuberosum* protein; active peptides; angiotensin-I-converting enzyme; dipeptidyl peptidase-IV;

Introduction

Obesity, diabetes, and hypertension are significant metabolic disorders that substantially increase the risk of cardiovascular diseases, commonly known as silent killers [1, 2]. Furthermore, there is a close interconnection between diabetes and hypertension through shared metabolic pathways, resulting in an increased likelihood of coexistence in individuals [3, 4]. Angiotensin-converting enzyme (ACE; EC 3.4.15.11) and dipeptidyl peptidase-IV (DPP-IV; EC 3.4.14.5) are two crucial enzymes involved in the regulation of blood pressure and blood glucose, respectively [5, 6]. Accordingly, the using DPP-IV and ACE inhibitors has emerged as promising therapeutic approaches for managing type 2 diabetes and hypertension, respectively, resulting in significant reductions in blood glucose and blood pressure levels.

Bioactive peptide therapy has gained recognition as a potential treatment option due to its limited side effects compared to synthetic drugs and its effectiveness in curing patients [7, 8]. Regularly, peptides have demonstrated medical efficacy in various organisms, exhibiting antioxidant, anti-hypertensive, antidiabetic, and anti-inflammatory properties [9, 7]. Recent literature emphasizes the preference for discovering and researching active peptides with multiple functions rather than individual biological activity. This offers significant advantages in terms of providing convenient and efficient treatment for patients with multiple diseases over an extended period, in contrast to the regular approach. For instance, peptides with ACE and DPP-IV inhibitory activities have been identified in dietary proteins such as broccoli [10], buffalo milk [11], and *Picrorhiza kurroa* [12] hydrolysates.

Chinese chive (*Allium tuberosum Rottler*. ex Spreng or *A. tuberosum*), well-known as a vegetable, has been widely consumed in food and traditional medicine with a long history [13]. *A. tuberosum* seeds have been reported their chemical constituents containing alkaloids,

steroidal saponions, and amides. Moreover, rats have been observed to have a positive activity on their sexual behavior after supplement oral administered *A. tuberosum* seeds extract for 40 days [13]. Furthermore, Chinese chive crude extracts have properties relating to antioxidant and antimicrobial effects [14]. To discover more biological activities of Chinese chive seeds, the present study focused on isolating and characterizing the active peptides with multiple functions connecting to anti-diabetes and anti-hypertension activities derived from the hydrolysate of *A. tuberosum*. Various proteases were applied to hydrolyze Chinese chive seed proteins to generate peptides with short sequencings. The hydrolysates' activities were evaluated using in vitro ACE and DPP-IV inhibitory assays. The potent active peptides in the most active hydrolysate were further uncovered using the bioassay-guided fractionation to give the most active fraction. Moreover, the peptide sequences in this fraction were determined using liquid chromatography-tandem mass spectrometry (LC-MS/MS) combined with de novo sequencing. The peptides were synthesized using solid-phase synthesis according to corresponding identified sequences and then their IC_{50} values were determined for the assessment of the peptides' biological activities. The molecular mechanism and structural stability of DPP-IV and ACE inhibitory peptides were studied through peptide inhibition kinetics using the Lineweaver-Burk plot and pre-incubation experiments, respectively. Additionally, docking simulations were also performed to understand the interactions between active peptides and the DPP-IV and ACE, respectively.

Results and Discussion

The biological inhibitory activity of different Chinese chives' hydrolysates

A. tuberosum seed protein hydrolysates generated by thermolysin, trypsin, pepsin, chymotrypsin, and a combination GI enzyme (gastrointestinal simulation enzymes containing pepsin, trypsin, and α-chymotrypsin) were examined for ACE and DPP-IV inhibitory activities,

showing significantly different inhibitory effects of hydrolysates. The ACE and DPP-IV inhibitory effects of hydrolysates were analyzed based on their IC_{50} values.

For dual-functional biological activities, the thermolysate hydrolysate obtained the highest inhibitory activity to the best one for ACE inhibitory activity (the IC_{50} value of 26.26 ± 0.77 µg/mL) and the third strong for DPP-IV (the IC_{50} value of 4.86 ± 0.27 mg/mL) inhibitory effect as compared to the remaining hydrolysates (**Table 1** and Supplementary data **Figure S1**). Then, pepsin hydrolysate performed the second position due to the best to against DPP-IV enzyme with the IC_{50} value of 3.43 ± 0.54 mg/mL and the worst activity to inhibit ACE enzyme with the IC_{50} value of 317.50 ± 141.50 mg/mL. As the third potential rank, GI hydrolysate showed the IC_{50} values of 5.49 ± 0.48 mg/mL and 108.40 ± 9.07 µg/mL for DPP-IV and ACE inhibitory activities, respectively. After that, α-chymotrypsin and trypsin hydrolysates performed less strong than above hydrolysates. α-Chymotrypsin exhibited the ACE and DPP-IV inhibitory activities with the IC_{50} values of 36.75 ± 0.81 µg/mL and 5.93 ± 0.98 mg/mL, respectively. Trypsin displayed the effects to prevent ACE enzyme (IC_{50}: 317.50 ± 141.50 µg/mL) and DPP-IV enzyme (63.49 ± 28.53 mg/mL).

Bioassay-guided fractionations of *A. tuberosum* hydrolysates

The *A. tuberosum* seed hydrolysates digested by thermolysin and GI enzymes were further fractionated using RP-HPLC, based on the superior DPP-IV and ACE inhibitory activity of the thermolysin hydrolysate (as shown in **Table 1**), and the GI hydrolysate which simulated the in vivo gastrointestinal digestion. The bioactive peptides generated through the action of digestive enzymes in the gastrointestinal (GI) tract exhibited resilience against the digestive enzymes present in the GI tract upon oral consumption, enabling the peptides to retain their intact structure [10]. Actually, target peptides are absorbed as an oral health supplement, and they undergo digestion and hydrolyzation under controlling of enzymes from the human gastrointestinal tract. Peptides released from Trypsin, Chymotrypsin, and Pepsin hydrolysates

are prone to fragmentation following digestion in the gastrointestinal tract. These resulting peptide fragments are similar to those generated by the hydrolyzation of gastrointestinal digestive enzymes. Therefore, this study selected peptides with inhibitory activity from the hydrolysates of thermolysin and GI (even though the pepsin hydrolysate showed the better inhibitory activities of GI hydrolysate). Recently, GI enzymes were widely applied to generate bioactive peptides from natural protein sources, for example peptides derived from soft-shell turtle yolk [15], Chinese Rushan and Naizha cheese [16], and cooked beef, pork, chicken and turkey meat [17].

As depicted in **Figures 1**, the thermolysin and GI hydrolysates were separated for 60 minutes and collected every 5 min, yielding 12 fractions (F1-F12). These fractions were analyzed using in vitro DPP-IV and ACE inhibitory assays to determine the fraction with the best inhibitory activity. For the ACE inhibitory effect, fractions F6, F7, and F8 of the thermolysin hydrolysate and fractions F6, F7, F8, and F9 of the GI hydrolysate showed greater inhibitory activity than the remaining fractions (**Figure 2A**). Additionally, for DPP-IV inhibitory activity, fractions F6, F7, and F8 of both hydrolysates were found to have the greatest effect among the twelve fractions (**Figure 2B**).

Identification of The Peptide Sequences

After conducting in vitro ACE and DPP-IV inhibitory assays, the active fractions (F6, F7, F8, and F9) obtained from RP-HPLC were selected for peptide sequencing under LC-MS/MS, utilizing a scanning range of m/z 150-1200. The LC-MS/MS raw data were processed using Mascot Distiller software, employing a database-assisted sequencing approach with the *Allium tuberosum* database downloaded from the NCBI. However, it is important to note that the genome for chive seed has not been fully decoded, resulting in incomplete protein and peptide information available on NCBI. This limitation hinders precise peptide identification.

Hence, alongside database comparison, the de novo sequencing software PEAKS Studio 8.5 was utilized to determine the peptide sequences.

From the thermolysin hydrolysate fractions, eight peptides were identified, while twenty-two peptides were isolated from the GI hydrolysate fractions **(Table 2)**. **Figure 3A** displays the chromatogram and mass spectrum of the hydrolysate analyzed by LC-MS/MS. The highest signal mass-to-charge ratios (m/z) of 592.3 and 701.4 were detected at 29.90 minutes and 30.28 minutes, respectively. One identical peptide, with m/z 592.3 was identified between the thermolysin and GI hydrolysates **(Figure 3B)**. The sequences LLPSY (LY-5) (m/z of 592.3) were determined by PEAKS Studio 8.5, and the MS/MS mass spectra of this peptide sequence was depicted in **Figure 3B and 3D**. The identified product ions of b ions and y ions readily matched the predicted fragments of the corresponding sequence. Moreover, heptapeptide NAPALVY (m/z of 701.4), only released from GI hydrolysate, was also selected for further investigation due to its appearance in the second-highest peak (t_R=30.28 minutes) in the LC-MS chromatogram of GI fraction 7 **(Figure 3A, C and E)** and the high percentage of hydrophobic residues (Leu, Ala, Pro, Val) in its sequence which are usually recognized in ACE and DPP-IV inhibitory peptides.

For analysis the ACE and DPP-IV inhibitory effects, peptides LY-5 and NY-7 were further chemically synthesized. The synthetic peptides LY-5 and NY-7 were also used to confirm the peptide sequences identified in GI hydrolysate, as depicted in Supplementary data **Figures S3 and S4**. Two selective ion chromatograms (m/z 592.3) obtained from GI fraction 7 and synthetic LY-5 exhibited similar retention times (t_R) of 18.98 and 19.06, respectively (Supplementary data **Figure S3A**), along with comparable MS/MS fragment distributions (Supplementary data **Figure S3B**). Similarly, two selective ions (m/z 747.4) achieved from GI fraction 7 and synthetic NY-7 showed similar retention times (t_R) of 19.03 and 19.09 in their respective chromatograms (Supplementary data **Figure S4A**), along with two comparable

MS/MS fragment patterns (Supplementary data **Figure S4B)**. These findings provide compelling evidence confirming the sequence of these candidate peptides.

Distinguishing between the isomers Ile (I) and Leu (L) can be challenging due to their identical molecular weight. In the case of the peptide sequence LLPSY, it could also potentially be IIPSY, LIPSY, and ILPSY. To resolve this ambiguity, four pentapeptides, LLPSY, IIPSY, LIPSY, and ILPSY, were chemically synthesized. Their retention times in the hydrolysate were compared (data not shown). The retention time of the mass-to-charge ratio in LLPSY and the hydrolysate was nearly identical, while other three peptides exhibited a noticeable difference. Consequently, the peptide sequence was determined to be LLPSY, following the identification made by PEAKS Studio.

Bioactivities of Peptides Through in Vitro Assay

After synthesis, peptides LY-5 and NY-7 were used to determine their biological activities and their IC_{50} values against ACE and DPP-IV were calculated using GraphPad Prism 5.0 (GraphPad Software, Inc.) at different concentrations of peptides. As shown in **Table 1** and Supplementary data **Figure S2A and S2B**, the IC_{50} value of LY-5 obtained 15.66 ± 1.11 μM while NY-7 achieved the IC_{50} value of 3.42 ± 0.79 μM for inhibiting ACE. Similarly, the in vitro DPP-IV assays were also carried out to calculate the IC_{50} value of LY-5 and NY-7. As displayed in **Table 1** and Supplementary data **Figure S2C and S2D**, the IC_{50} values of LY-5 and NY-7 were respectively achieved at 2.48 ± 0.10 mM and 7.63 ± 0.52 mM for against DPP-IV enzyme.

Until now, there has been a significant annual increase in the number of peptides derived from natural protein sources that possess multiple functional biological activities, particularly in terms of their ACE and DPP-IV inhibitory effects. In a study conducted by Gu et al., five novel peptides were identified through in silico proteolysis of buffalo milk proteins. Two peptides (KPW and RGP) exhibited ACE inhibitory effects with IC_{50} values of 136.28 ±

10.77 μM and 104.72 ± 8.37 μM, respectively, as well as DPP-IV inhibitory effects (KPW, FPK, and KFTW) with IC_{50} values of 82.52 ± 10.37 μM, 126.57 ± 8.45 μM, and 873.92 ± 32.89 μM, respectively [11]. Moreover, the umami peptide IPIPATKT, obtained from Sanhuang chicken hydrolysate, demonstrated potential as a peptide with IC_{50} values of 265 μM and 64 μM for ACE and DPP-IV inhibitory activities, respectively [18]. Furthermore, among the 65 peptides identified from *Picrorhiza kurroa* Royle ex Benth hydrolysate, the peptide ASGLCPEEAVPRR exhibited excellent dual ACE (IC_{50} value of 43.40 μM) and DPP-IV (IC_{50} value of 2.2 μM) inhibitory activities [12]. Another excellent example is the peptides produced from Broccoli hydrolysate, which showed ACE inhibitory activities with IC_{50} values of 0.776 ± 0.03 μM (LPGVLPVA) and 8.52 ± 0.63 μM (YLYSPAY), as well as DPP-IV inhibitory activities with IC_{50} values of 392 ± 24 μM (LPGVLPVA) and 181 ± 4 μM (YLYSPAY). Additionally, the in vivo experiments indicated that rats and mice administered with Broccoli hydrolysate peptides exhibited significant effects on regulating blood pressure and blood glucose levels [10].

Interestingly, the pentapeptide LLPSY has not only been isolated from chive seed hydrolysate but has also been identified in olive seed hydrolysate, which is associated with antioxidant properties and antihypertensive capacity [19, 20]. Subsequently, a synthetic peptide LLPSY exhibited ACE inhibitory activity with an IC_{50} value of 39.9 ± 0.5 μM [19], which appears to be higher than our current result of 15.66 ± 1.11 μM. Although their study focused solely on analyzing the IC_{50} value of LLPSY, further investigation is still required to fully understand the characteristic action of this peptide [19, 20].

According to the previous publications, the highly potent effects of the ACE and DPP-IV inhibitory peptides are regularly contributed by the presence of several specific residues, the high hydrophobic amino acids, and short sequences [21, 22]. Moreover, the C-terminus and N-terminus of peptide sequences were determined to play primary roles in inhibiting the ACE

and DPP-IV activity, respectively [5, 1]. These findings are consistent with the ability of peptides to possess multiple biological effects. In the present study, peptides LY-5 (LLPSY) and NY-7 (NAPALVY) have possessed a tyrosine residue (aromatic amino acids) at their C-terminal sequence that is linked to the promising inhibiting ACE ability [21]. The good ACE inhibitory activity of pentapeptide LY-5 may also be supported by the presence of leucine at the N-terminal end [23]. Additionally, hydrophobic amino acids such as Ile, Leu, Ala, Pro, Val, Gly, Phe, Met, and Trp were detected in both ACE and DPP-IV inhibitory peptides [22, 21, 24]. Notably, the sequences of LY-5 and NY-7 contained high hydrophobic residues (Ile, Leu, Ala, Pro, Val), contributing to their inhibitory ability for ACE and DPP-IV enzymes. Furthermore, the DPP-IV enzyme is known to specifically remove dipeptides from the N-terminus of polypeptides with the structure Xaa-proline and Xaa-alanine, which is recognized in the sequence of NY-7 (NAPALVY) [25, 5, 26]. Overall, these findings suggest that the identified peptides from *A. tuberosum* hydrolysates have promising potential for controlling hypertension and type 2 diabetes through their ACE and DPP-IV inhibitory activities.

Peptide Inhibition Patterns of ACE and DPP-IV

Enzyme inhibitors are commonly classified into four types based on their mechanisms of action: competitive, noncompetitive, uncompetitive, and mix-type [25]. The Km (Michaelis constant) and Vmax (maximum reaction velocity) values for peptides LY-5 and NY-7 were shown in Supplementary data **Table S1**. This study examined the inhibitory kinetics of LY-5 and NY-7 against ACE using a Lineweaver- Burk plot with substrate HHL (2.5mM, 1mM, 0.5mM, 0.2mM, 0.1mM, and 0.05mM) and varying concentrations of the synthetic peptides. **Figure 4A** shows that for LY-5, three straight lines intersected at the same point on the 1/S axis, indicating that it acts as a noncompetitive inhibitor of ACE. In the noncompetitive inhibitor mode, the Km value remains constant while the Vmax value decreases with increasing peptide concentration (Supplementary data **Table S1**). In this case, the inhibitory peptide does

not directly affect the interaction between the enzyme and its substrate. However, the presence of the inhibitory peptide reduces the availability of functional enzymes, consequently diminishing the overall enzymatic activity. As a result, the ability of the substrate concentration to be effectively protected is enhanced. Typically, noncompetitive inhibitors bind to non-active sites on the enzyme, rather than directly interacting with its catalytic sites like competitive inhibitors. In contrast, NY-7 exhibited a distinct behavior, where three sets of peptides with varying concentrations intersected at a single point on the 1/Vi axis (**Figure 4B**). This observation indicates that NY-7 acts as a competitive inhibitor of ACE. As a competitive inhibitor, NY-7 has the capability to directly compete with the ACE substrate for binding to the active sites of the enzyme. By doing so, it effectively prevents the substrate from being cleaved by the enzyme.

To determine the DPP-IV inhibitory modes of LY-5 and NY-7, a Lineweaver-Burk plot was employed, utilizing varying concentrations of the GP-pNA substrate in the presence and absence of the peptides **(Figure 4C, D)**. The obtained results indicated that LY-5 exhibited no significant difference in the Vmax value across concentrations of 0, 1.67, and 3.33 mM. This finding suggests that LY-5 functions as a competitive inhibitor, capable of interacting with the catalytic sites of DPP-IV (Supplementary data **Table S1** and **Figure 4C**). Notably, competitive inhibition mechanisms are widely observed in DPP-IV inhibition patterns and are considered a prevalent mode of action [25]. For instance, four DPP-IV inhibitory peptides derived from quinoa hydrolysate with potential IC_{50} values (IPI: 5.25 μM; IPV: 26.15 μM; VAYPL: 42.93 μM; IPIN: 56.58 μM) have been identified as competitive inhibitors [27]. Moreover, DPP-IV competitive inhibitory peptides were also determined in napin of rapeseed *(Brassica napus)* hydrolysate (IPQVS) [28], camel whey protein (VPV, YPI, VPF, EPVK, LAHKPL, YPLR) [29], and mouse lymphocytes (SGVSLAALKKALAAAGYDVEK) [30]. On the other hand, peptide NY-7 was found to be a noncompetitive inhibitor of DPP-IV, as its Km value remained

stable in both situations, whether NY-7 was present or absent (Supplementary data **Table S1** and **Figure 4D)**. It suggests that NY-7 has been interacted with DPP-IV receptor via the second binding sites instead of directly binding with the active sites. Until now, the DPP-IV noncompetitive inhibitors were widely common, such as peptides obtained from α-lactalbumin-rich whey hydrolysate (LDQWLCEKL, IC_{50}: 131 μM) [31], Atlantic salmon skin hydrolysate (VLATSGPG, IC_{50}: 1.73 mM) [32], and mouse lymphocytes (SAPRHGSLGFLPRK, IC_{50}: 23.443 mg/L) [30]. These findings clarify the inhibitory mechanisms of LY-5 and NY-7 against DPP-IV, demonstrating their potential as therapeutic agents for diseases such as diabetes.

Stability of ACE and DPP-IV inhibitory peptides

Peptides that inhibit ACE and DPP-IV activity can be categorized into three types based on their stability against enzymes: real-substrate, prodrug, and true inhibitor [33, 34]. In a pre-incubation test, the true inhibitor type remains unchanged in its ACE and DPP-IV inhibitory activities, while the real-substrate type shows a reduction in activity, and the prodrug type exhibits an increase in activity. As shown in **Figure 5A**, the ACE inhibitory effects of LY-5 were slightly reduced from 53.1% to 38.6% without and with pre-incubated ACE, respectively. Moreover, LC-MS was further investigated to analyze fragment products of this pre-incubation experiment. As anticipated, LY-5 (LLPSY, m/z 592.07) was hydrolyzed by ACE into a small fragment as LLP (m/z 341.94) (**Figure 6**). It indicated that LY-5 is a real substrate of ACE. Unlike LY-5, peptide NY-7 was not significantly different in its ACE inhibitory activity comparing between with (37 %) and without (36.3%) pre-incubated with ACE, suggesting that NY-7 acts as a true inhibitor of ACE (**Figure 5B**).

No significant differences in the DPP-IV inhibitory activities were observed between LY-5 and NY-7, whether pre-incubated with DPP-IV or not. This suggests that both LY-5 and NY-7 are true inhibitors of DPP-IV (**Figure 5C, D**). Furthermore, previous studies have

reported that peptides containing Pro or Hyp at the third position from the N-terminus (known as the P1' position) are resistant to DPP IV cleavage [26, 35]. This finding aligns with our stability results, indicating that LLPSY and NAPALVY are unlikely to be hydrolyzed by DPP-IV.

Molecular docking study of LY-5 and NY-7 peptide to ACE and DPP-IV receptors

The molecular simulation was applied to predict the interactions of peptides LY-5 and NY-7 with ACE and DPP-IV under the calculation of Accelrys Discovery Studio 3.0 software. The crystal structures of ACE (1O86.pdb) and DPP-IV (1WCY.pdb) were selected as the target proteins for the simulations. The simulation analysis involved the determination of binding sites, interaction bonds, and energy calculations for the peptide-enzyme complexes. In particular, the CDOCKER energy score was used as a measure of the quality of molecular interactions between the peptides and the ACE and DPP-IV receptors. A lower binding energy indicates a more favorable and stable molecular conformation between the peptides and the respective ACE and DPP-IV receptors.

The ACE enzyme typically contains three main binding pockets, known as S1, S2, and S1', within its active sites [36, 12]. The S1 pocket, comprised of Ala354, Glu384, and Tyr523 residues, is relatively narrower compared to the S2 pocket, which includes Glu281, His353, Lys511, His513, and Tyr520 residues. The S1' pocket, on the other hand, consists of the Glu162 residue. Moreover, the ACE crystal structure possesses an additional active site where zinc ion (Zn^{2+}) coordination takes place with His383, His387, and Glu411 residues. As shown in **Figure 7A**, peptide NY-5 has made bonds to the second binding sites instead of the active pockets of ACE, suggesting this peptide acts as a noncompetitive inhibitor of ACE. This result was consistent with our present kinetic analysis. The CDOCKER energy of pentapeptide NY-5 interacting with ACE was calculated at -69.3661 kcal/mol. Peptide NY-5 has formed 2 pi-pi bonds to ACE via His410 (2.9 Å) and Arg124 (5.4 Å). Moreover, the complex of NY-5 and

ACE was produced by five hydrogen bonds at Arg520 (2.4 Å), Asn66 (2.4 Å), Asn70 (2.3 and 2.4 Å), and Glu134 (3.3 Å).

The docking study indicated that peptide NY-7 interacted with ACE through active sites which agrees with our mechanism study, proving that NY-7 acts as a competitive inhibitor of ACE. Heptapeptide NY-7 interacted closely with Tyr523 (2.1 Å) in the S1 pocket, Gln281 (2.0 Å), Lys511 (2.3 Å), and Tyr520 (2.1 and 2.5 Å) in the S2 pocket, His383 (2.4 Å) in the zinc-binding motif HEXXH **(Figure 7B)**. Further, NY-7 also formed with ACE via non-active sites at Asn66 (2.1 and 2.5 Å) and Glu403 (2.2 Å). Nine hydrogen bonds were observed in the NY-7 and ACE complex and no pi-pi interaction. The CDOCKER energy of NY-7 binding with ACE was lower than that of LY-5 (-69.3661 kcal/mol) at - 84.39 kcal/mol, seeming it is the reason explain for the higher ACE inhibitor of NY-7 (the IC_{50} value of 3.42 ± 0.79 μM) as compared to that of LY-5 (the IC_{50} value of 15.66 ± 1.11 μM).

According to the findings of previous studies, DPP-IV exhibits three distinct active pockets [37, 38]. The first pocket, known as the S1 pocket, is composed of Val656, Trp659, Tyr631, Tyr662, Tyr666, and Val711 residues. Additionally, DPP-IV possesses the S2 pocket, which consists of Glu205, Glu206, Arg125, Arg358, Phe357, Tyr662, Ser209, and Val207 residues. Furthermore, DPP-IV showcases a catalytic triad that includes Ser630, Asp708 (or Asn710), and His740 residues. In **Figure 7C**, the results reveal that LY-5 demonstrates the highest affinity for the DPP-IV domain with a CDOCKER energy of -55.423 kcal/mol. Notably, the N-terminal Leucine residue of LY-5 enters the activation region of DPP-IV and forms a hydrogen bond with Tyr662 in the DPP-IV S1 activation region, while also establishing a pi bond with Tyr666. Furthermore, LY-5 exhibits a charged interaction with Glu205 in the DPP-IV S2 activation region, connecting with Glu206 of DPP-IV through two hydrogen bonds and charged interactions. Additionally, the C-terminal Tyrosine residue of LY-5 engages in a hydrogen bond and a pi-π bond interaction with Lys-554 and Arg-560 of DPP-IV, respectively.

In **Figure 7D**, it is observed that NY-7 demonstrates the highest affinity for the DPP-IV domain at coordinates x, y, z = 44.854, 56.633, 29.945, with a CDOCKER energy of -79.3838 kcal/mol. Notably, the N-terminal Asparagine residue of NY-7 exhibits both a charge interaction and a hydrogen bond interaction with Arg471 of DPP-IV. Additionally, the Valine residue of NY-7 forms a hydrogen bond with Val459. The molecular docking results of ligand LY-5 and NY-7 and DPP-IV receptor were consistent with the Lineweaver-Burk plot analysis mentioned above and confirmed that LY-5 and NY-7 act as a competitive inhibitor and a non-competitive inhibitor of DPP-IV enzyme, respectively.

Quantitative analysis of the peptides in *A. tuberosum* protein hydrolysate

LY-5 and NY-7 are two promising peptides that have shown potential for inhibiting both ACE and DPP-IV activities. While these peptides have been identified in *A. tuberosum* protein hydrolysate, it is crucial to determine the precise quantities of these compounds in parent protein to utilize this valuable information in product development and quality control. By accurately measuring the levels of these peptides, manufacturers can better understand the potential therapeutic benefits of their products and ensure consistent quality over time. In the present study, these peptides were quantitatively analyzed in *A. tuberosum* GI hydrolysate employing LC-MS/MS with multiple reaction monitoring (MRM) modes. Under the monitoring of LC-MS/MS, six concentrations of synthetic peptides with a range of 5-500pg/µl were analyzed to establish the standard calibration curve with a linear regression equation (y = ax+b). For the LY-5 peptide, a linear regression equation (y = 112510x - 32136) and R_2 of 0.9996 (correlation coefficient) were generated using this peptide with a transition m/z 592.3 > 366.1 at a collision energy of 19V (Supplementary data **Figure S5A**). Similarly, synthetic peptide NY-7 with a transition m/z 746.2 > 282.1 at a collision energy of 42V was used to build a linear regression equation (y = 254.57x - 2171) with an R_2 of 0.9993 (Supplementary data **Figure S5B**).

The weight of LY-5 and NY-7 peptides were calculated in GI hydrolysate (Supplementary data **Figure S6)**. According to MRM results, the content of LY-5 in chive seeds, protein, and hydrolyzate contents were 13.39 μg/g, 142.87 μg/g, and 476.25 μg/g; the ones of NY-7 were 89.94 μg/g, 874.30 μg/g and 2914.43 μg/g (**Table 3**). It can be seen that the content of NY-7 in chive seeds is significantly higher than that of LY-5.

Conclusion

A. tuberosum hydrolysates generated from thermolysin and GI (gastrointestinal simulation) hydrolysates were proven potent ACE and DPP-IV inhibitory activities. In particular, two novel ACE inhibitory peptides, LLPSY (LY-5) and NAPALVY (NY-7), were identified with IC_{50} values of 15.66 ± 1.11 μM and 3.42 ± 0.79 μM, respectively. The Lineweaver-Burk plot and pre-incubation test revealed that LY-5 functions as a noncompetitive mode and a real substrate, while NY-7 acts as a competitive mode and true inhibitor of ACE. Additionally, both LY-5 and NY-7 demonstrated DPP-IV inhibitory activities with IC_{50} values of 2.48 ± 0.10 mM and 7.63 ± 0.52 mM and acted as competitive and noncompetitive inhibitors against DPP-IV, respectively. Notably, both peptides are true inhibitors of DPP-IV. The presence of LY-5 and NY-7 in chive seed protein hydrolyzate was quantified, with NY-7 being particularly abundant. Overall, *A. tuberosum* seed protein hydrolysate possesses an excellent ability to produce multiple functional peptides that have potential blood pressure and blood sugar lowering effects.

Materials and Methods

Chemical and Reagents

The following chemicals and reagents were used in this study: human Dipeptidyl-peptidase-IV (DPP-IV), Gly-Pro-p-nitroaniline (GP_pNA), linagliptin, angiotensin-I-converting enzyme (ACE, from rabbit lungs), hippuryl-L-histidyl-L-leucine (HHL), hippuric acid (HA), ferulic acid, Captopril, Sodium hydroxide (NaOH), Sodium lauryl sulfate (SDS),

thermolysin (from *Geobacillus stearothermophilus*), trypsin (from bovine pancreas), pepsin (from porcine gastric mucosa), α-chymotrypsin (from bovine pancreas), dimethyl sulfoxide (DMSO), N,N'-diisopropylcarbodiimide (DIC), triisopropylsilane (TIS), ethyl ether from Sigma Chemical Co. (St. Louis, MO, USA). Additionally, ammonium bicarbonate (ABC), acetonitrile (ACN), formic acid (FA), tris hydrochloride (Tris-HCl), trichloroacetic acid (TCA), piperidine, and boric acid were purchased from J.T. Baker (Phillipsburg, NJ, USA). Trifluoroacetic acid (TFA), N,N-diisopropylethylamine (DIPEA), and 4-methylmorpholine (NMM) were obtained from Alfa Aesar (Lancashire, UK). o-(Benzotriazol-1-yl)- N,N,N',N' -tetramethyluronium hexafluorophosphate (HBTU) was produced by Chem-Impex Int'l. Inc. (Wood Dale, IL, USA), and Wang resin was obtained from Cleo Salus (Louisville, KY, USA). Deionized water (ddH_2O) was prepared using the PURELAB® water purification system from ELGA LabWater (Lane End, High Wycombe, UK).

Protein preparation

The extraction of Chinese chive seed protein was performed using a modified version of a previously established protocol [39]. A solution of 1% SDS was used to disperse the *A. tuberosum* powder, which was then homogenized using an ultra-sonicator homogenizer (Branson Digital Sonifier®, CA, USA) at 30% amplitude, with the 30s/20s on/off pulse repeated four times. Throughout the extraction process, the sample was kept chilled on ice to preserve the integrity of the proteins. After centrifugation at 1,000 rpm for 15 minutes, the resulting supernatant was collected. To precipitate the protein, a mixture of 20% TCA in acetone was added at a 3:1 (v/v) ratio to the supernatant and incubated at 4°C for 3 hours. The precipitated pellets were then washed with ddH_2O and centrifuged at 1,000 rpm for 5 minutes before being lyophilized for subsequent hydrolysis.

Preparation of *A. tuberosum* protein hydrolysate

A. tuberosum protein was hydrolyzed with different enzymes at the same ratio of sample/enzyme (w/w, weight/weight) of 1/25 at each suitable temperature condition for specific enzyme activity. Trypsin, chymotrypsin, and pepsin hydrolysis were performed at the optimal temperature of 37°C, while thermolysin digestion was carried out at 60°C. Pepsin was activated in a buffer containing 10% methanol and its pH value was adjusted to 1.9 using HCl, while the remaining enzymes were performed in 25 mM ABC (ammonium bicarbonate) at pH 8.0. After incubation time for 16 hours, the hydrolysis reaction was stopped by keeping the hydrolysate at -20°C.

Moreover, small peptides were also generated by multiple enzymes as gastrointestinal simulation enzymes (Trypsin, Chymotrypsin, and Pepsin) into 2 steps. Firstly, the protein sample at pH 1.9 was incubated with pepsin at 37°C for 10 hours. The product of the reaction was lyophilized to prepare for the second time of enzyme digestion. Secondly, the lyophilized peptic hydrolysate was dissolved in 25 mM ABC at pH 8.0 and hydrolyzed with trypsin and chymotrypsin at 37°C for another 10 hours. The short-chain peptides were collected using a 3kDa ultrafiltration membrane combined with a centrifuged step at 14,000rpm for 15 minutes and then lyophilized hydrolysate for subsequent use.

Fractionation using reversed-phase high performance liquid chromatography (RP-HPLC)

The desalted hydrolysates with a smaller size (< 3kDa) were fractionated using RP-HPLC (Hitachi Chromaster, Tokyo, Japan). A C_{18} column (4.6mm x 250mm, particle size 5µm; Thermo Scientific Inc., Rockwood, TN, USA) was employed for this purpose. The samples were dissolved in a buffer containing 5% ACN and 0.1% FA. A linear gradient was applied using mobile phase A (5% ACN and 0.1% TFA) and mobile phase B (95% ACN and 0.1% TFA) at a flow rate of 1 mL/min for a total of 60 minutes. The gradient started with 0% B for the initial 5 minutes, followed by a gradual increase to 30% B over the next 40 minutes.

Subsequently, buffer B was increased to 80% over 5 minutes, and then a flush was performed for 5 minutes. Finally, buffer B was decreased to 0% for the last 5 minutes. During this process, twelve fractions (F1-F12) were collected at 5-minute intervals on the chromatogram, and the wavelength at 214 nm was monitored.

LC-MS/MS analysis of peptides in the active fractions

The active fractions exhibiting potential DPP-IV and ACE inhibitory activity were selected for analysis using the Ultimate 3000 RSLC system (Dionex, Sunnyvale, CA, USA) with a C_{18} column (150mm × 2.1mm, 3μm, Thermo Scientific) and the Thermo Q-Exactive™ mass spectrometer (Thermo Scientific Inc., USA). The fractions were dissolved in a solution containing 5% ACN and 0.1% FA. Mobile phase A consisted of 0.1% FA in water, while mobile phase B comprised 95% ACN and 0.1% FA. The analysis was conducted using a linear gradient at a flow rate of 250 μL/min, lasting for 75 minutes. The elution gradient proceeded as follows: (i) 1% mobile phase B was maintained for the initial 4 minutes; (ii) mobile phase B was gradually increased to 5% over the next 6 minutes; (iii) between 10 and 15 minutes, mobile phase B was further increased to 10%; (iv) a 5-minute step was taken to increase mobile phase B to 80% to ensure complete elution of any remaining sample in the column, and this concentration was maintained for 10 minutes; (v) finally, mobile phase B was decreased to the initial concentration of 1% over 3 minutes and maintained for 7 minutes to allow for multiple sample analyses during automatic sampling.

Protein identification and peptide sequencing

The RAW data (the tandem MS data) were saved to MGF file format and analyzed using Mascot Distiller v2.3.2.0 (Matrix Science, London, UK) software for database search, as well as Peak Studio (version 8.5, Bioinformatics Solutions Inc., Waterloo, ON, Canada) software for de novo search. In the Mascot Distiller software, the parameters were configured as follows: (i) the enzyme digestion used was the same as in the experiment; (ii) the protein

database of *Allium tuberosum* obtained from NCBI (the National Center for Biotechnology Information; www.ncbi.nlm.nih.gov) was selected; (iii) the enzymatic hydrolysis allowed a cut-off error of one amino acid; (iv) the peptide and MS/MS tolerance were set to 10 ppm and 0.1 Da, respectively; (v) a significance hit threshold of $p<0.05$ was chosen.

For software PEAKS studio 8.5, the de novo search parameters were selected including: (i) select the enzyme and protein modification used in the protein hydrolyzates; (ii) the error ranges of MS were set to 10 ppm; (iii) MS/MS tolerance was set 0.1 Da. The sequences of identified peptides were validated using manual MS/MS assignment and confirmed by comparison with retention time, m/z values, and MS/MS spectra of the corresponding synthetic peptides.

Solid-phase peptide synthesis

Solid-phase synthesis using a microwave-assisted reactor (CEM Microwave Technology Ltd., Buckingham, UK) was performed to prepare more peptide amounts for further studies. The peptides were synthesized one by one residue from the C-terminal to the final residue of the N-terminal sequence according to the identified sequences. The peptide synthesis protocol was applied following our previous report [40]. After that, synthesized peptide sequences were validated by the LC-MS/MS as described in above section (LC-MS/MS analysis of peptides in the active fractions). The purity of peptides was enhanced using RP-HPLC with a suitable gradient for specific peptides.

Determination of ACE inhibitory activity

The in vitro ACE inhibitory assay was described based on reported method of Cushman with minor modification [41]. Samples used as inhibitors were dissolved in 1% DMSO solution while ACE and HHL were liquefied in sodium borate buffer containing 200 mM borate buffer and 300 mM NaCl at pH 8.3. Firstly, 10 µL of sample was preincubated with 30 µL of 2.5 mM HHL solution at 37°C for 5 minutes (min). Secondly, the mixture was added 20 µL of 2 U/µL

ACE solution and monitored at 37°C for 30 min, following another half hour at the same temperature at 200 rpm by a shaker incubator. However, captopril and borate buffer were used for positive control and blank instead of sample, respectively. Thirdly, the reaction was stopped using 60 µL of 1N HCl.

The peak area of HHL and its hydrolyzed product Hippuric acid (HA) were analyzed by HPLC (Hitachi Chromaster, Japan) equipped with a C_{18} column (4.6mm x 250mm, 5µm, Macherey-Nagel, Düren, Germany). The products of ACE reaction were isolated using a single gradient with 80% mobile phase A (5% ACN and 0.1% TFA) and 20% mobile phase B (95% ACN and 0.1% TFA) solution at a flow rate of 1 mL/min elute for 15 minutes. The UV wavelength was control at 228 nm. ACE inhibition rate (%) is calculated as follows:

$$\text{ACE Inhibition (\%)} = \left[1 - \frac{\Delta\text{A inhibitor}}{\Delta\text{A control}}\right] \times 100\%$$

The $\Delta A_{inhibitor}$ and $\Delta A_{control}$ were the peak area of hippuric acid existed in the reaction solution with and without inhibitor. The calculation of the IC_{50} value was based on the samples with five different concentrations to calculate the ACE inhibition rate (%) and predict it with the nonlinear regression analysis method.

Determination of DPP-IV inhibitory activity

The in vitro DPP-IV inhibitory assay was carried out according to the reported procedure of Lacroix and Li-Chan under the monitoring of SpectraMax 190 Microplate Reader (Molecular Devices, LLC, San Jose, CA, USA) at a wavelength of 405 nm [42]. Samples were dissolved in a 1% DMSO solution and used as inhibitors. The positive control was linagliptin, and the substrate of the DPP-IV enzyme was GP-pNA (Gly-Pro p-nitroanilide hydrochloride). The assay involved pre-incubating 25 µL of 2mM NaOH with the same volume of 1.6mM substrate GP-pNA at 37°C for 10 minutes. After that, 25 µL of DPP-IV buffer and 25 µL of the sample were added to the mixture solution and maintained at 37°C for another 10 minutes.

The reaction was then carried out using 50 µL of 1U/µL DPP-IV and incubated at the same temperature for an hour. The experiment was terminated by adding 100 µL of 1M Sodium acetate with a pH value of 4.

$$\text{DPPIV Inhibition (\%)} = \left[1 - \frac{\Delta \text{OD}_{405\text{nm}}\ \text{inhibitor} - \text{Blank}}{\Delta \text{OD}_{405\text{nm}}\ \text{control} - \text{Blank}}\right] \times 100\%$$

The DPP-IV inhibition rate (%) was calculated using the formula provided, and the IC_{50} value was predicted using nonlinear regression analysis based on the absorbance values of five different concentrations of samples.

Investigation of inhibition patterns of ACE and DPP-IV inhibitory peptides

To determine the inhibition mechanisms of ACE and DPP-IV inhibitory peptides, the methodologies described in above section (determination of ACE and DPP-IV inhibitory activity) were followed with some modifications, respectively. Different concentrations of substrates, such as HHL (2.5mM, 1mM, 0.5mM, 0.2mM, 0.1mM, and 0.05mM) for ACE and GP-pNA (1.6mM, 1.2mM, 1mM, 0.5mM, 0.2mM, and 0.1mM) for DPP-IV, were used in the absence and presence of varying concentrations of the inhibitory peptides. The reciprocal of the HHL and GP-pNA concentration was plotted on the X-axis (1/[S]), and the measured signal area was calibrated against the HA and pNA calibration line to calculate the production amount of the HHL product (HA) and the GP-pNA product (pNA). The required production per unit production time (hr/mM) was used as the Y-axis to generate a pair of reciprocal curves, known as a Lineweaver-Burk plot. The intersection position of the three straight lines was observed, and the Vmax and Km values were calculated as the basis for confirming the interaction between ACE and DPP-IV and the target peptides.

Stability of ACE inhibitory peptides under ACE hydrolysis

The synthesized peptides were evaluated their stability against ACE according to the method of Shih et. al. with slight modification [40]. Each peptide (10 µL in ddH_2O) was incubated with ACE (20 µL at a concentration of 0.05 mU/µL) at 37°C for 3 hours.

Subsequently, a mixture of 30 μL of 2.5 mM HHL substrate was added, and the reaction was allowed to proceed at 37°C for 30 minutes with shaking at 200 rpm. The reaction was stopped by adding 60 μL of 1N HCl, and the ACE inhibitory activity of the peptides was determined using the method described in Section of determination of ACE inhibitory activity.

Stability of DPP-IV inhibitory peptides towards DPP-IV hydrolysis

The stability of LY-5 and NY-7 against DPP-IV enzymes was assessed as following our published method with a minor modification [15]. Each peptide (25 μL) was combined with DPP-IV (50 μL at a concentration of 1 U/μL) in 25 μL of DPP-IV buffer, and the mixture was incubated at 37°C for 3 hours. Following the incubation, the reaction mixture was supplemented with 25 μL of 2 mM NaOH and an equal volume of 1.6 mM GP-pNA, and further incubated at 37°C for 60 minutes. To halt the reaction, 100 μL of sodium acetate (pH 4) was added. The inhibitory effects of LY-5 and NY-7 against DPP-IV were then determined using the method described in Section of determination of DPP-IV inhibitory activity.

Docking simulation

The molecular-level interactions between ligands (investing peptides) and receptors (target enzymes) were analyzed using the software Discovery Studio V.3.0 (Accelrys Software, Cambridge, UK). The structures of peptides were obtained using the same software. The crystal structures of human ACE (1O86.pdb, resolution 2.0 Å) [36] and DPP-IV (1WCY.pdb, resolution 2.2 Å) [37] were downloaded from the RCSB PDB (Protein Data Bank; www.rcsb.org). The binding energy was calculated under controlling of CHARMm (Chemistry at HARvard Macromolecular Mechanics) program. The surrounding water molecules were removed from the 3D structure of ACE and DPP-IV enzymes before the processing of the docking simulation. The docking environment was adjusted to pH 8.3 and pH 8.0 for simulating with in vitro ACE assay and DPP-IV assay, respectively. The docking parameters were set up with cavity detection with a radius of 31.2 Å (the coordinates x: 39.0592, y: 37.9168, z:

50.1074) for LY-5 and NY-7 in binding to ACE. Similarly, the docking analyses for the DPP-IV receptor were completed with the coordinates x, y, z = 44.854: 56.633: 29.945 (cavity detection with a radius of 16 Å) for NY-7 and x: y: z = 55.616: 62.198: 36.883 (cavity detection with a radius of 14 Å) for LY-5.

Quantification of LY-5 and NY-7 in gastrointestinal simulation digest of *A. tuberosum* proteins

LY-5 and NY-7 peptides present in chive seeds protein hydrolysate and GI hydrolysate were qualified using LC-MS/MS with multiple reaction monitoring (MRM) modes (TSQ, Thermo Scientific). Synthetic standard peptides were dissolved in a solution of ddH_2O containing 5% ACN and 0.1% FA, with concentrations ranging from 5 ng/μL to 1000 ng/μL, to create standard calibration curves. MRM transitions for LY-5 and NY-7 were set at m/z 592.3 > 366.1 (collision-induced dissociation energy of 19 V) and m/z 746.2 > 282.1 (collision-induced dissociation energy of 42 V), respectively. The mobile phases used were: mobile phase A (5% ACN and 0.1% FA in ddH_2O) and mobile phase B (95% ACN and 0.1% FA in ddH_2O). Separation was achieved using an ODS Hypersil column (150 mm × 2.1 mm, 5 μm, Thermo Scientific) with an elution gradient over 20 minutes at a flow rate of 0.350 mL/min. The gradient consisted of a 5-minute initial hold at 5% buffer B, followed by a 5-minute increase from 5% to 80% buffer B, a 5-minute hold at 80% buffer B, and a final 5-minute isocratic hold at 5% buffer B. The analysis was performed in positive mode with the following parameters: capillary temperature of 300°C, auxiliary gas pressure of 5 arb, sheath gas pressure of 40 arb, tube lens offset of 124 V, and a spray voltage of 3.5 kV.

Data analysis

In this study, the results were processed using GraphPad Prism 9.0 (GraphPad Software, Inc., La Jolla, CA, USA) and presented as the mean standard deviation from triplicate analyses.

Supplementary Information The online version contains supplementary material available at https://doi.org/

Funding

This study received financial support from the National Science and Technology Council (NSTC 112-2113-M-020-001), Taiwan.

Acknowledgments

We would like to express our gratitude to the Precision Instrument Center of NPUST and Mithra Biotechnology Inc. for their invaluable assistance with the mass spectrometry analysis.

Author contributions

Nhung Thi Phuong Nong: Writing - original draft, Data curation, Formal analysis, Conceptualization, Writing - review & editing; Chia-Hui Lee: Writing - original draft, Investigation, Formal analysis, Conceptualization; Jue-Liang Hsu: Conceptualization, Investigation, Methodology, Software, Writing - review & editing, Supervision, Funding acquisition.

Compliance with ethical standards

Conflicts of interest

The authors declare no conflict of interest.

References

1. Majumder K, Wu J. Molecular targets of antihypertensive peptides: understanding the mechanisms of action based on the pathophysiology of hypertension. Int J Mol Sci. 2015;16(1):256-83. https://doi.org/10.3390/ijms16010256

2. Brouwers S, Sudano I, Kokubo Y, Sulaica EM. Arterial hypertension. The Lancet. 2021;398(10296):249-61. https://doi.org/10.1016/S0140-6736(21)00221-X

603 3. Abouelkheir M, El-Metwally TH. Dipeptidyl peptidase-4 inhibitors can inhibit angiotensin
604 converting enzyme. European journal of pharmacology. 2019;862:172638.
605 https://doi.org/10.1016/j.ejphar.2019.172638
606 4. Cheung BM, Li C. Diabetes and hypertension: is there a common metabolic pathway? Curr
607 Atheroscler Rep. 2012;14(2):160-6. https://doi.org/10.1007/s11883-012-0227-2
608 5. Andersen ES, Deacon CF, Holst JJ. Do we know the true mechanism of action of the DPP-
609 4 inhibitors? Diabetes Obes Metab. 2018;20(1):34-41. https://doi.org/10.1111/dom.13018
610 6. Udenigwe CC, Mohan A. Mechanisms of food protein-derived antihypertensive peptides
611 other than ACE inhibition. J Funct Foods. 2014;8:45-52.
612 https://doi.org/10.1016/j.jff.2014.03.002
613 7. Udenigwe CC, Aluko RE. Food protein-derived bioactive peptides: production, processing,
614 and potential health benefits. J Food Sci. 2012;77(1):R11-R24.
615 https://doi.org/10.1111/j.1750-3841.2011.02455.x
616 8. Gourgari E, Wilhelm EE, Hassanzadeh H, Aroda VR, Shoulson I. A comprehensive review
617 of the FDA-approved labels of diabetes drugs: Indications, safety, and emerging
618 cardiovascular safety data. J Diabetes Complicat. 2017;31(12):1719-27.
619 https://doi.org/10.1016/j.jdiacomp.2017.08.005
620 9. Möller NP, Scholz-Ahrens KE, Roos N, Schrezenmeir J. Bioactive peptides and proteins
621 from foods: indication for health effects. Eur J Nutr. 2008;47(4):171-82.
622 https://doi.org/10.1007/s00394-008-0710-2
623 10. Zhou T, Liu Z, Pei J, Pan D, Gao X, Dang Y et al. Novel Broccoli-Derived Peptides
624 Hydrolyzed by Trypsin with Dual-Angiotensin I-Converting Enzymes and Dipeptidyl
625 Peptidase-IV-Inhibitory Activities. J Agric Food Chem. 2021;69(37):10885-92.
626 https://doi.org/10.1021/acs.jafc.1c02985

627 11. Gu Y, Li X, Qi X, Ma Y, Chan ECY. In silico identification of novel ACE and DPP-IV
628 inhibitory peptides derived from buffalo milk proteins and evaluation of their inhibitory
629 mechanisms. Amino Acids. 2023;55(2):161-71. https://doi.org/10.1007/s00726-
630 02203202-z
631 12. Thakur S, Chhimwal J, Joshi R, Kumari M, Padwad Y, Kumar R. Evaluating peptides of
632 picrorhiza kurroa and their inhibitory potential against ACE, DPP-IV, and oxidative stress.
633 J Proteome Res. 2021;20(8):3798-813. https://doi.org/10.1021/acs.jproteome.1c00081
634 13. Guohua H, Yanhua L, Rengang M, Dongzhi W, Zhengzhi M, Hua Z. Aphrodisiac
635 properties of *Allium tuberosum* seeds extract. J Ethnopharmacol. 2009;122(3):579-82.
636 https://doi.org/10.1016/j.jep.2009.01.018
637 14. Chen C, Cai J, Ren Y-H, Xu Y, Liu H-l, Zhao Y-y et al. Antimicrobial activity, chemical
638 composition and mechanism of action of Chinese chive *(Allium tuberosum Rottler)*
639 extracts. Front Microbiol. 2022:4349. https://doi.org/10.3389/fmicb.2022.1028627
640 15. Nong NTP, Chen Y-K, Shih W-L, Hsu J-L. Characterization of Novel Dipeptidyl
641 Peptidase-IV Inhibitory Peptides from Soft-Shelled Turtle Yolk Hydrolysate Using
642 Orthogonal Bioassay-Guided Fractionations Coupled with In Vitro and In Silico Study.
643 Pharmaceuticals. 2020;13(10):308. https://doi.org/10.3390/ph13100308
644 16. Shi Y, Wei G, Huang A. Simulated in vitro gastrointestinal digestion of traditional Chinese
645 Rushan and Naizha cheese: Peptidome profiles and bioactivity elucidation. Food Res Int.
646 2021;142:110201. https://doi.org/10.1016/j.foodres.2021.110201
647 17. Martini S, Conte A, Tagliazucchi D. Comparative peptidomic profile and bioactivities of
648 cooked beef, pork, chicken and turkey meat after in vitro gastro-intestinal digestion. J
649 Proteomics. 2019;208:103500. https://doi.org/10.1016/j.jprot.2019.103500

650 18. Chen M, Pan D, Zhou T, Gao X, Dang Y. Novel umami peptide IPIPATKT with dual
651 dipeptidyl peptidase-IV and angiotensin I-converting enzyme inhibitory activities. J Agric
652 Food Chem. 2021;69(19):5463-70. https://doi.org/10.1021/acs.jafc.0c07138
653 19. Vásquez-Villanueva R, Muñoz-Moreno L, Carmena MJ, Marina ML, García MC. In vitro
654 antitumor and hypotensive activity of peptides from olive seeds. J Funct Foods.
655 2018;42:177-84. https://doi.org/10.1016/j.jff.2017.12.062
656 20. Esteve C, Marina M, García M. Novel strategy for the revalorization of olive (Olea
657 europaea) residues based on the extraction of bioactive peptides. Food Chem.
658 2015;167:272-80. https://doi.org/10.1016/j.foodchem.2014.06.090
659 21. Sasaki C, Tamura S, Tohse R, Fujita S, Kikuchi M, Asada C et al. Isolation and
660 identification of an angiotensin I-converting enzyme inhibitory peptide from pearl oyster
661 (Pinctada fucata) shell protein hydrolysate. Process Biochem. 2019;77:137-42.
662 https://doi.org/10.1016/j.procbio.2018.11.017
663 22. Nongonierma AB, FitzGerald RJ. Inhibition of dipeptidyl peptidase IV (DPP-IV) by proline
664 containing casein-derived peptides. J Funct Foods. 2013;5(4):1909-17.
665 https://doi.org/10.1016/j.jff.2013.09.012
666 23. García-Mora P, Martín-Martínez M, Bonache MA, González-Múniz R, Peñas E, Frias J et
667 al. Identification, functional gastrointestinal stability and molecular docking studies of
668 lentil peptides with dual antioxidant and angiotensin I converting enzyme inhibitory
669 activities. Food Chem. 2017;221:464-72. https://doi.org/10.1016/j.foodchem.2016.10.087
670 24. Wang R, Lu X, Sun Q, Gao J, Ma L, Huang J. Novel ACE inhibitory peptides derived from
671 simulated gastrointestinal digestion in vitro of sesame (Sesamum indicum L.) protein and
672 molecular docking study. Int J Mol Sci. 2020;21(3):1059.
673 https://doi.org/10.3390/ijms21031059

25. Nong NTP, Hsu J-L. Characteristics of Food Protein-Derived Antidiabetic Bioactive Peptides: A Literature Update. Int J Mol Sci. 2021;22(17):9508. https://doi.org/10.3390/ijms22179508

26. Mentlein R. Dipeptidyl-peptidase IV (CD26)-role in the inactivation of regulatory peptides. Regul Pept. 1999;85(1):9-24. https://doi.org/10.1016/S0167-0115(99)00089-0

27. You H, Wu T, Wang W, Li Y, Liu X, Ding L. Preparation and identification of dipeptidyl peptidase IV inhibitory peptides from quinoa protein. Food Res Int. 2022;156:111176. https://doi.org/10.1016/j.foodres.2022.111176

28. Xu F, Yao Y, Xu X, Wang M, Pan M, Ji S et al. Identification and quantification of DPP-IV-inhibitory peptides from hydrolyzed-rapeseed-protein-derived napin with analysis of the interactions between key residues and protein domains. J Agric Food Chem. 2019;67(13):3679-90. https://doi.org/10.1021/acs.jafc.9b01069

29. Nongonierma AB, Cadamuro C, Le Gouic A, Mudgil P, Maqsood S, FitzGerald RJ. Dipeptidyl peptidase IV (DPP-IV) inhibitory properties of a camel whey protein enriched hydrolysate preparation. Food Chem. 2019;279:70-9. https://doi.org/10.1016/j.foodchem.2018.11.142

30. Wang J, Xie Y, Luan Y, Guo T, Xiao S, Zeng X et al. Identification and dipeptidyl peptidase IV (DPP-IV) inhibitory activity verification of peptides from mouse lymphocytes. Food Science and Human Wellness. 2022;11(6):1515-26. https://doi.org/10.1016/j.fshw.2022.06.009

31. Jia C-l, Hussain N, Obaroakpo JU, Pang X-y, Zhang S-w, Lu J et al. Generation and characterization of dipeptidyl peptidase-IV inhibitory peptides from trypsin-hydrolyzed α-lactalbumin-rich whey proteins. Food Chem. 2020;318:126333. https://doi.org/10.1016/j.foodchem.2020.126333

32. Jin R, Teng X, Shang J, Wang D, Liu N. Identification of novel DPP–IV inhibitory peptides from Atlantic salmon (Salmo salar) skin. Food Res Int. 2020;133:109161. https://doi.org/10.1016/j.foodres.2020.109161

33. Nongonierma AB, FitzGerald RJ. Susceptibility of milk protein-derived peptides to dipeptidyl peptidase IV (DPP-IV) hydrolysis. Food Chem. 2014;145:845-52. https://doi.org/10.1016/j.foodchem.2013.08.097

34. Khedr S, Martin M, Deussen A. Inhibitory efficacy and biological variability of tryptophan containing dipeptides on human plasma angiotensin converting enzyme activity. J Hypertens. 2015;4(198):2167-1095.1000198. https://doi.org/10.4172/21671095.1000198

35. Power O, Nongonierma A, Jakeman P, FitzGerald R. Food protein hydrolysates as a source of dipeptidyl peptidase IV inhibitory peptides for the management of type 2 diabetes. Proc Nutr Soc. 2014;73(1):34-46. https://doi.org/10.1017/S0029665113003601

36. Natesh R, Schwager S, Sturrock E, Acharya K. Crystal Structure of Human Angiotensin Converting Enzyme in complex with lisinopril. Nature; 2003. p. 551–4. https://doi.org/10.1038/nature01370

37. Hiramatsu H, Yamamoto A, Kyono K, Higashiyama Y, Fukushima C, Shima H et al. The crystal structure of human dipeptidyl peptidase IV (DPPIV) complex with diprotin A. Biol Chem. 2004;385(6):561-4. https://doi.org/10.1515/BC.2004.068

38. Li N, Wang L-J, Jiang B, Li X-q, Guo C-l, Guo S-j et al. Recent progress of the development of dipeptidyl peptidase-4 inhibitors for the treatment of type 2 diabetes mellitus. Eur J Med Chem. 2018;151:145-57. https://doi.org/10.1016/j.ejmech.2018.03.041

39. Priyanto AD, Doerksen RJ, Chang C-I, Sung W-C, Widjanarko SB, Kusnadi J et al. Screening, discovery, and characterization of angiotensin-I converting enzyme inhibitory peptides derived from proteolytic hydrolysate of bitter melon seed proteins. J Proteomics. 2015;128:424-35. https://doi.org/10.1016/j.jprot.2015.08.018

40. Shih Y-H, Chen F-A, Wang L-F, Hsu J-L. Discovery and study of novel antihypertensive peptides derived from Cassia obtusifolia seeds. J Agric Food Chem. 2019;67(28):7810-20. https://doi.org/10.1021/acs.jafc.9b01922

41. Cushman DW, Cheung H, Sabo E, Ondetti M. Design of potent competitive inhibitors of angiotensin-converting enzyme. Carboxyalkanoyl and mercaptoalkanoyl amino acids. Biochemistry. 1977;16(25):5484-91. https://doi.org/10.1021/bi00644a014

42. Lacroix IM, Li-Chan EC. Dipeptidyl peptidase-IV inhibitory activity of dairy protein hydrolysates. Int Dairy J. 2012;25(2):97-102. https://doi.org/10.1016/j.idairyj.2012.01.003

Table

Table 1. IC_{50} values of enzymatic hydrolysates, LY-5, and NY-7 peptide on DPP-IV and ACE

	IC_{50} value of ACE inhibitory	**IC_{50} value of DPP-IV inhibitory**
GI (gastrointestinal)	108.40 ± 9.07 μg/mL	5.49 ± 0.48 mg/mL
Thermolysin	26.26 ± 0.77 μg/mL	4.86 ± 0.27 mg/mL
Trypsin	90.21 ± 7.33 μg/mL	63.49 ± 28.53 mg/mL
Chymotrypsin	36.75 ± 0.81 μg/mL	5.93 ± 0.98 mg/mL
Pepsin	317.50 ± 141.50 μg/mL	3.43 ± 0.54 mg/mL
LLPSY (LY-5)	15.66 ± 1.11 μM	2.48 ± 0.10 mM
NAPALVY (NY-7)	3.42 ± 0.79 μM	7.63 ± 0.52 mM

739 **Table 2.** List of identified peptides discovered in active fractions derived Thermolysin and GI

740 hydrolysate using de novo and database analysis

741

Enzyme	Fraction	Sorce	Protein	t_R	m/z	Peptide sequence	Identified score	ALC* (%)
Thermolysin	6	De novo	-	23.93	526.206	VSEEDEQDT	-	65
				24.61	486.7912	AVMVVRNAL		54
				25.49	542.1923	VSEECCEDGL		59
	7	De novo		28.89	513.7827	AVPEEVLRN		90
				30.23	592.3348	LLPSY		67
				33.29	583.381	LLLPQ		52
	8	De novo		41.51	980.4918	LETSLTTDT		53
	9	De novo		36.78	617.365	LLPQF		54
GI	6	Database: Allium tuberosum	Maturase K, partial (chloroplast)	50.68	469.7283	INQLSNYS	22	-
			Cysteine synthase	29.8	638.3237	EIWKATDGKID	21	
			NADH-plastoquinone oxidoreductase subunit 5, partial	29.9	1060.553	QNLSLVNSSV	14	
		De novo	-	27.31	795.427	ASASVVVY	-	54
				28.02	805.4462	APASVVVY		58
				33.4	637.2841	ADADVF		52
	7	Database: Allium tuberosum	Cytochrome oxidase subunit I, partial (mitochondrion)	46.4	768.5266	LLLLSLP	33	-
			Cysteine synthase	31.95	874.489	DVTELIGK	32	
			Ribulose-1,5-bisphosphate carboxylase/oxygenase large subunit, partial (chloroplast)	54.31	387.2134	IDRQKN	20	
			NADH-plastoquinone oxidoreductase subunit 5, partial (chloroplast)	29.73	1060.554	QNLSLVNSSV	18	

	De novo	-	27.75	805.446	APGTVVVY	-	56
			28.47	681.8385	QSDNAMVSNLVGK		93
			28.66	681.8381	TNDNAMVSNLVGK		92
			29.76	592.3352	LLPSY		80
			30.28	747.4024	NAPALVY		61
			32.61	664.3331	LGEAGAF		54
			42.59	555.2509	ELMY		50
8	De novo	-	34.01	435.2578	QAGLTAVPL	-	58
			35.46	689.3624	ANLVSW		64
			36.91	617.3662	LLPQF		75
			50	672.3372	EGLAPW		55
9	De novo	-	32.49	479.2541	LEAF	-	50

* ALC: Average local confidence

744 **Table 3.** Contents of LY-5 and NY-7 in *A. tuberosum* seeds
745

Peptide	Amount in different level (μg/g)		
	In seed	In protein	In hydrolysate
LY-5	13.39 ± 0.11	142.87 ± 1.13	476.25 ± 3.77
NY-7	89.94 ± 5.08	874.30 ± 52.22	2914.43 ± 174.07

746

Figure

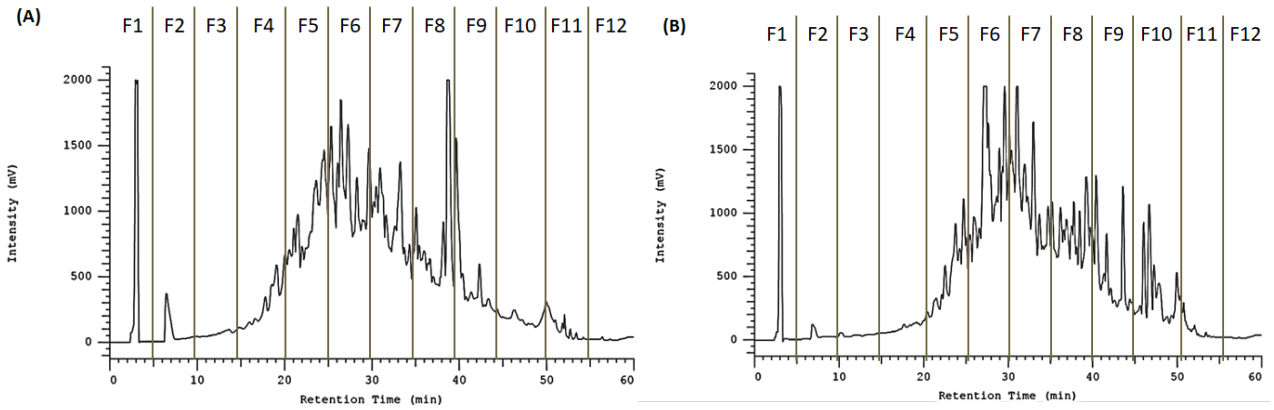
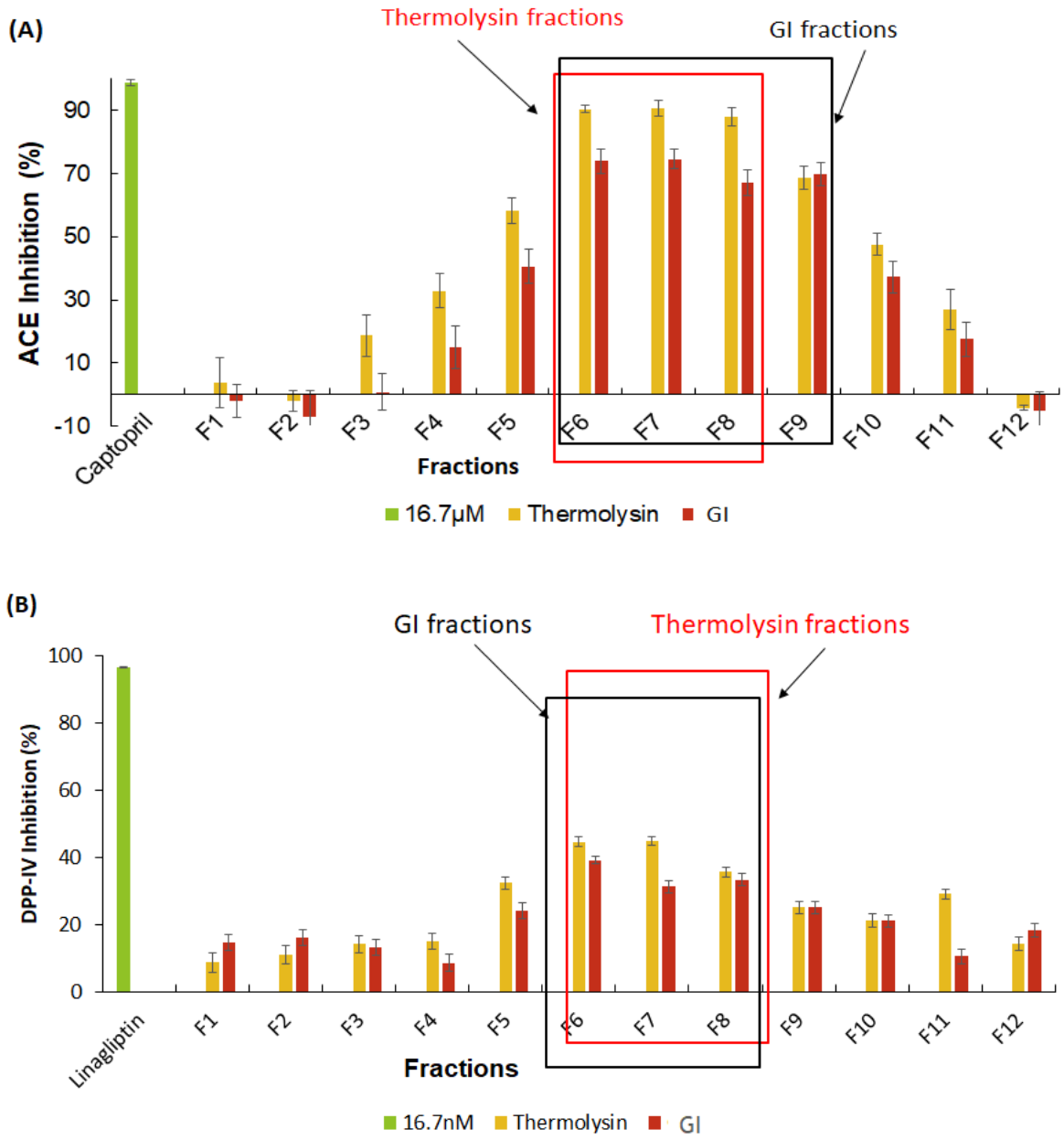


Figure 1. RP-HPLC chromatogram (A) thermolysin hydrolysate and (B) GI hydrolysate of *A. tuberosum* seed proteins

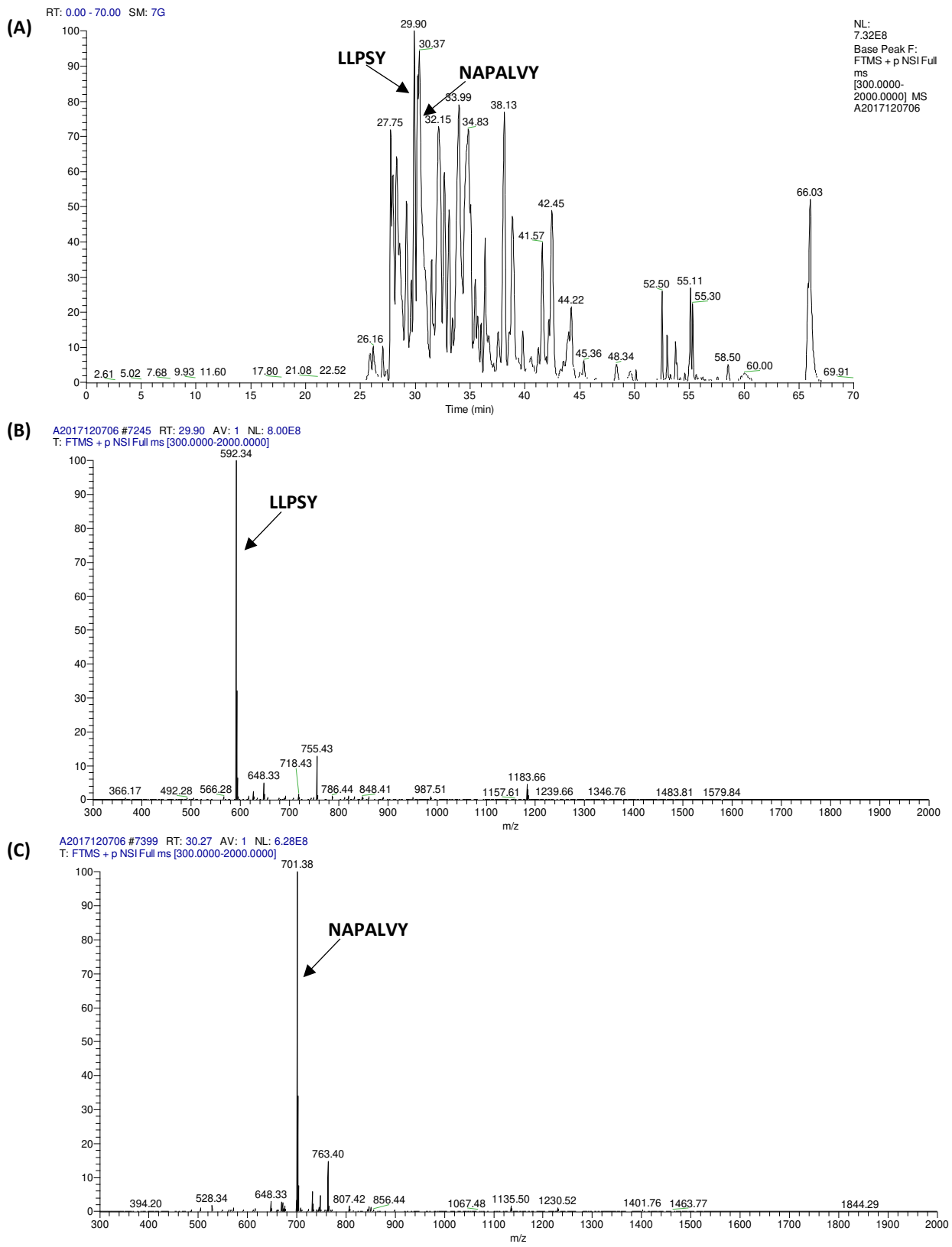


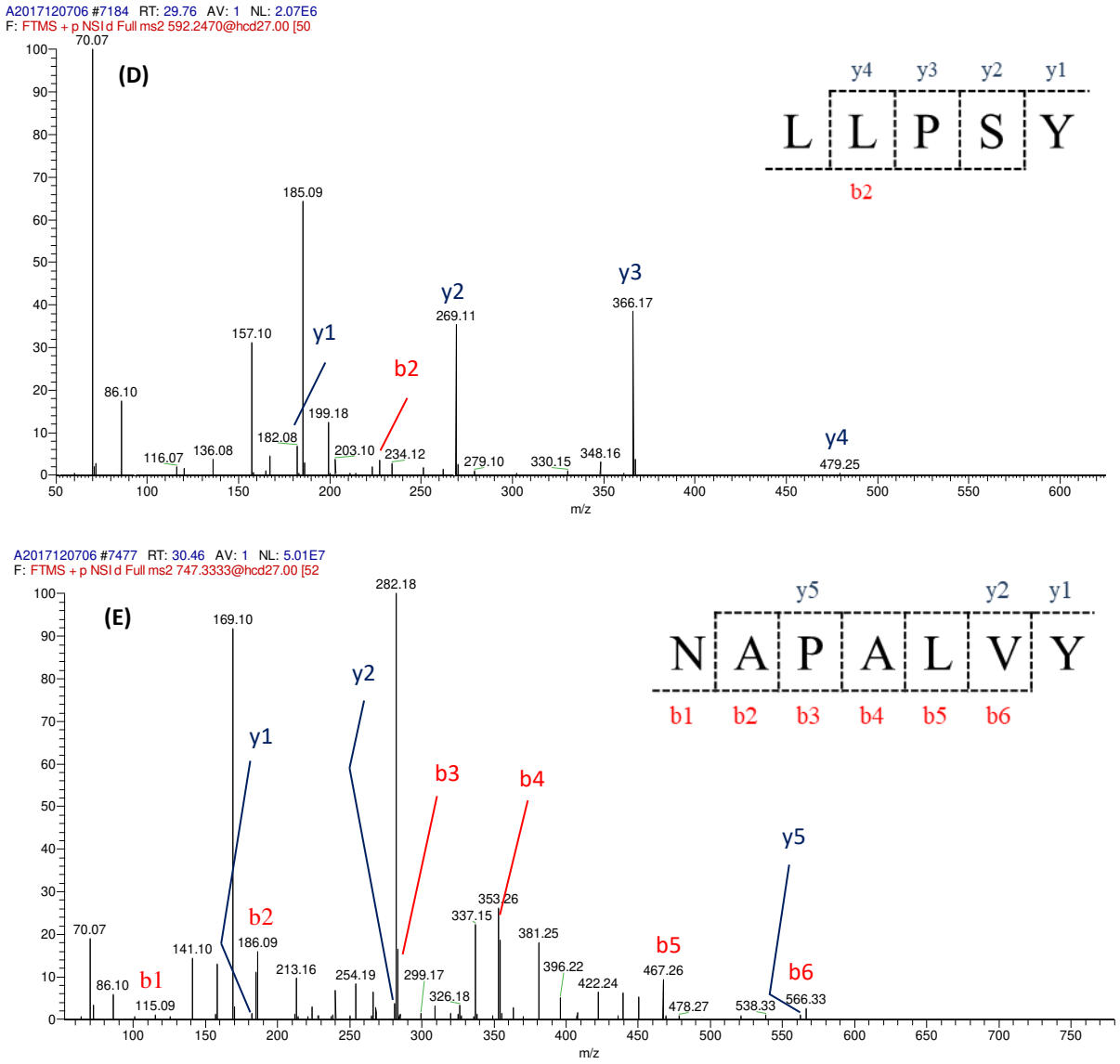
753

754 **Figure 2.** The inhibitory effects of fractions derived from thermolysin and GI hydrolysate

755 against (A) ACE and (B) DPP-IV.

756


(A)
RT: 0.00 - 70.00 SM: 7G
NL:
7.32E8
Base Peak F:
FTMS + p NSI Full
ms
[300.0000-
2000.0000] MS
A2017120706
LLPSY
NAPALVY
Time (min)
(B)
A2017120706 #7245 RT: 29.90 AV: 1 NL: 8.00E8
T: FTMS + p NSI Full ms [300.0000-2000.0000]
LLPSY
m/z
(C)
A2017120706 #7399 RT: 30.27 AV: 1 NL: 6.28E8
T: FTMS + p NSI Full ms [300.0000-2000.0000]
NAPALVY
m/z



767

768 **Figure 3.** LC-MS analysis of GI hydrolysate fraction 7. (A) LC-MS chromatogram of fraction

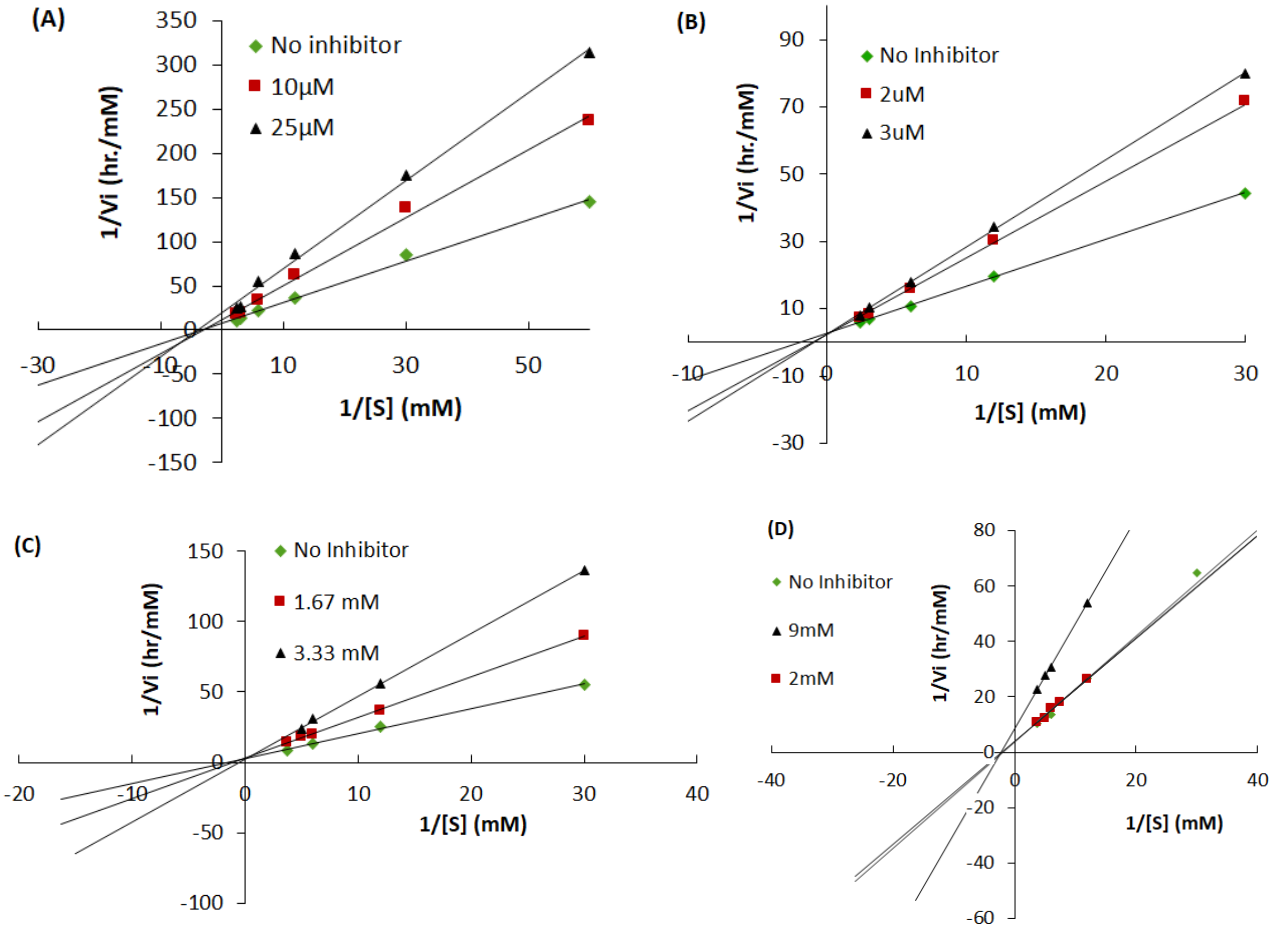
769 7; (B) MS spectrum at t_R= 29.9 min (C) and t_R= 30.28 min; (D) MS/MS spectrum of the ion

770 m/z 592.3 and (E) MS/MS spectrum of the ion m/z 747.4.

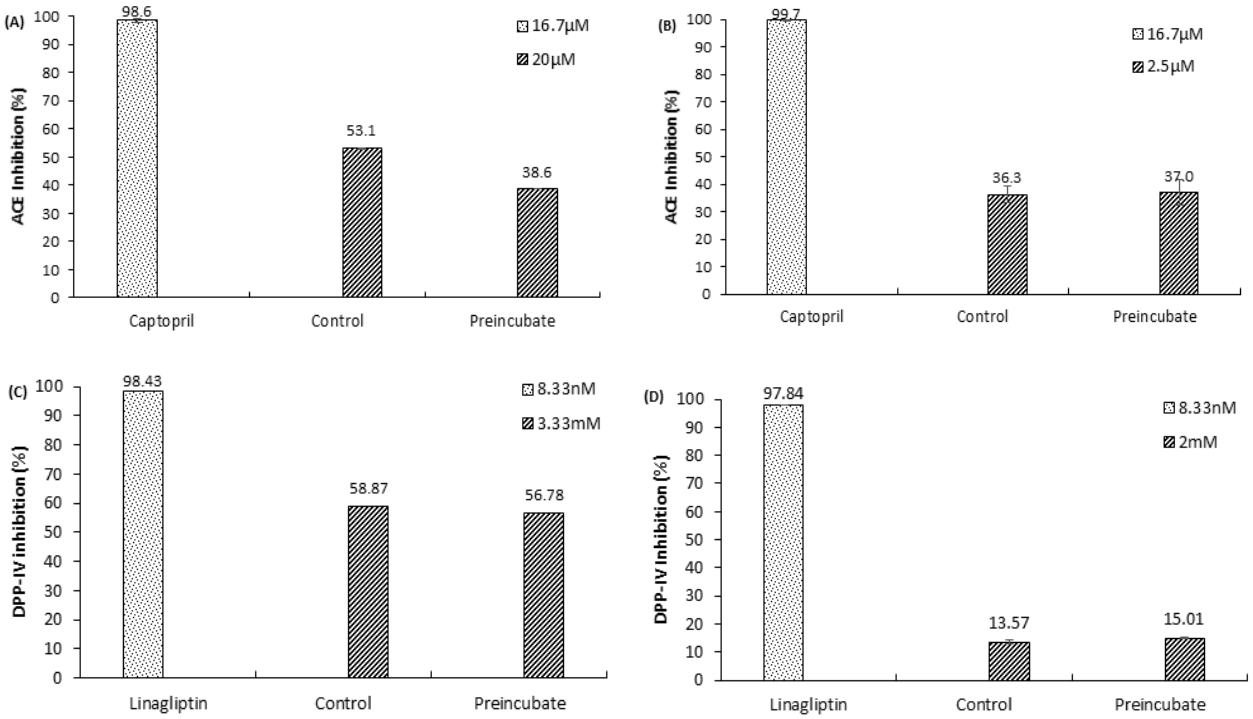
771

772

773



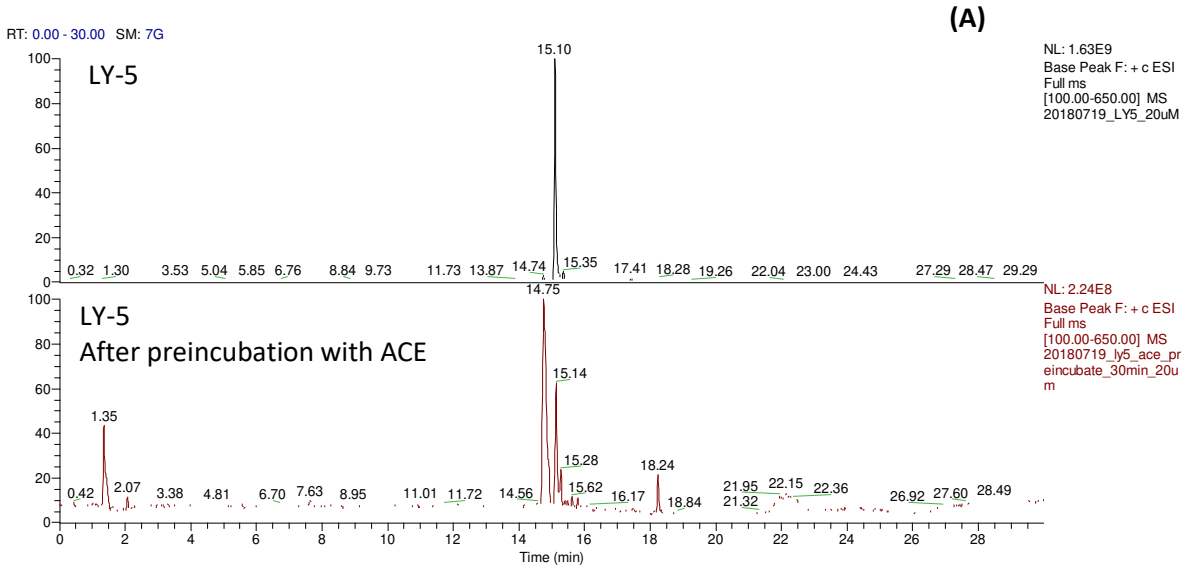
774
775
776 **Figure 4.** Lineweaver-Burk double reciprocal plots of (A) LY-5 (noncompetitive) and (B) NY-
777 7 (competitive) inhibition of ACE activity; (C) LY-5 (competitive) and (D) NY-7
778 (noncompetitive) inhibition of DPP-IV activity.
779



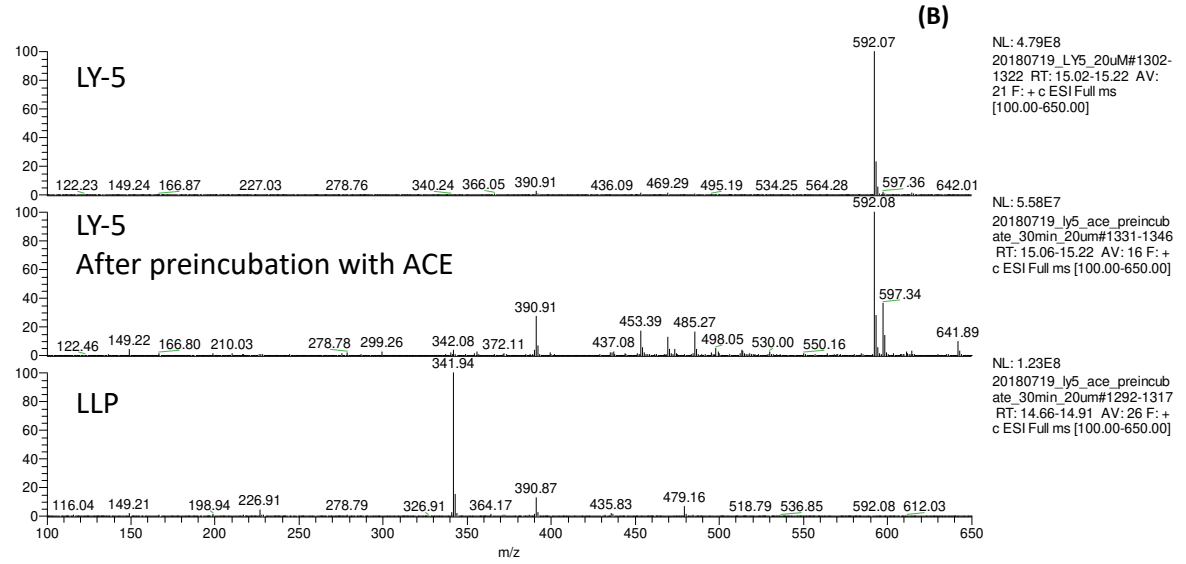
780

781 **Figure 5.** The inhibitor type determination of (A) LY-5 (B) NY-7 against ACE; the inhibitor
782 type determination (C) LY-5 (D) NY-7 against DPP-IV. Captopril and Linagliptin were used
783 as positive control for in vitro ACE and DPP-IV inhibitory assays, respectively. Peptide LY-5
784 and NY-7 without and with pre-incubated enzymes were used as control samples and
785 preincubate samples, respectively.

786



787



788

789 **Figure 6.** LC-MS analysis of LY-5 pre-incubated with ACE. (A) LC-MS chromatograms of

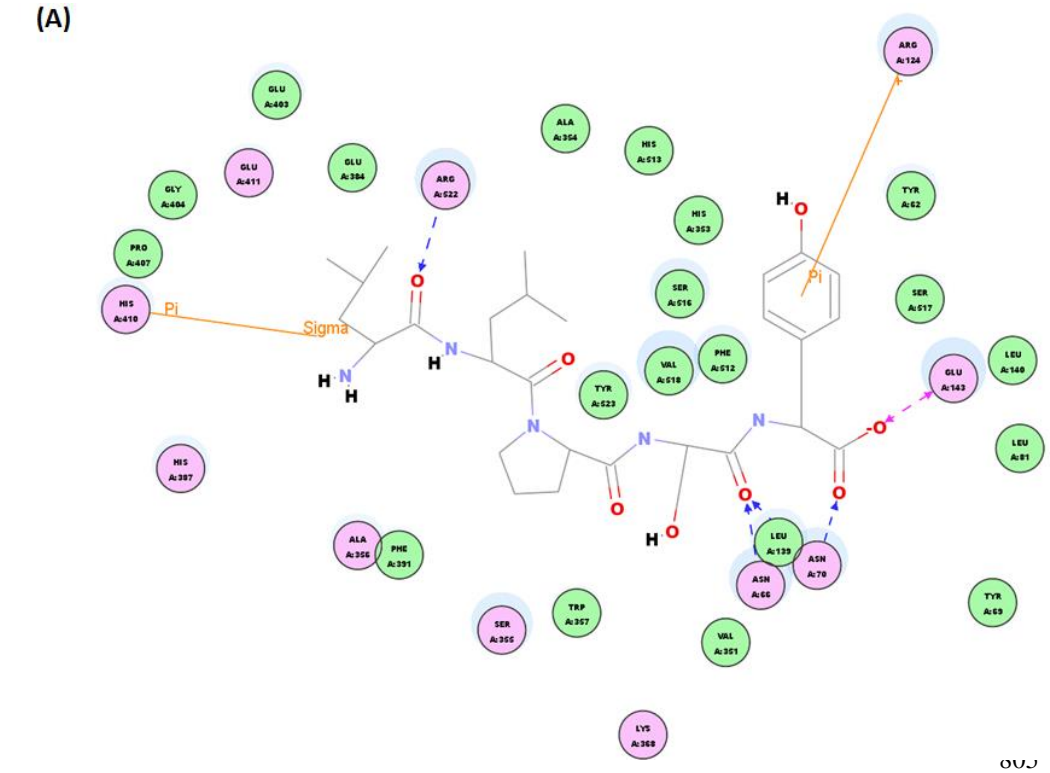
790 LY-5 with and without pre-incubated with ACE and (B) MS spectrum of LLP fragment (m/z

791 341.94) formed from LY-5 (m/z 592.07) cleaved by ACE.

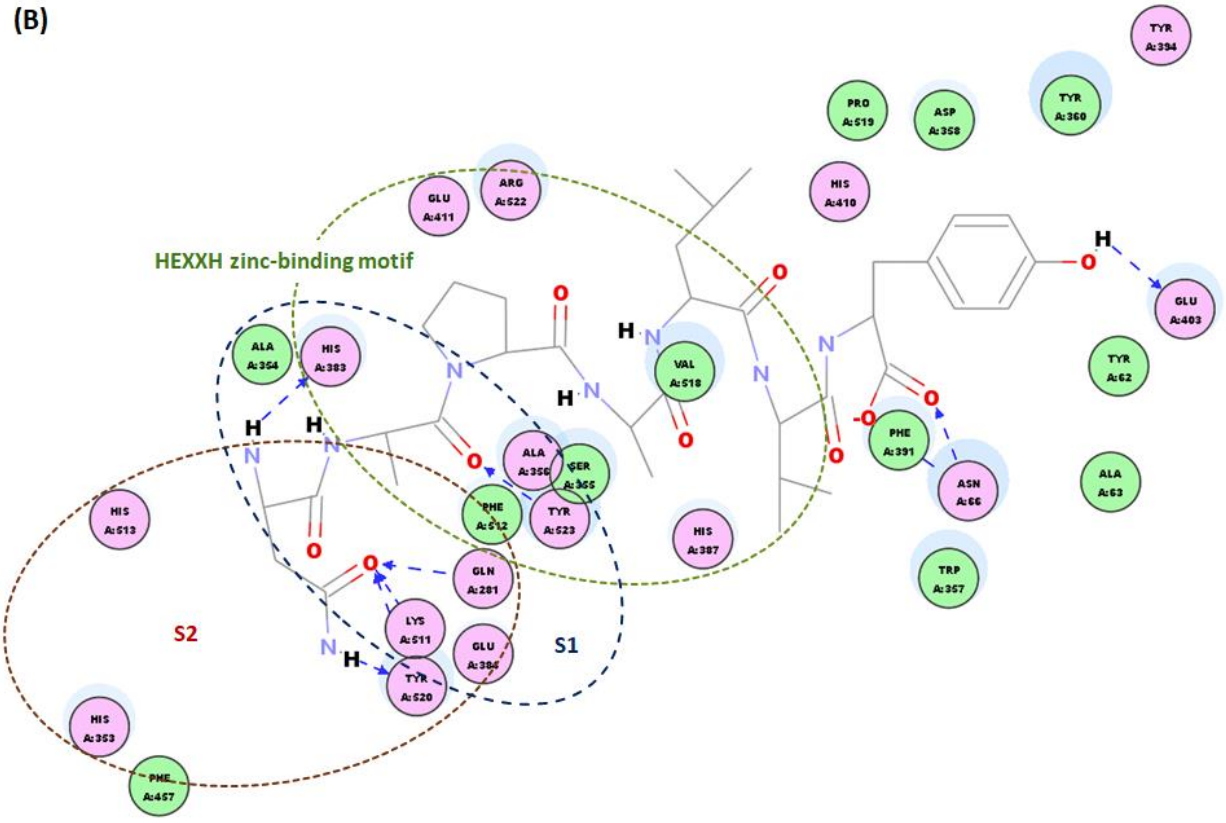
792

793

794



805



806

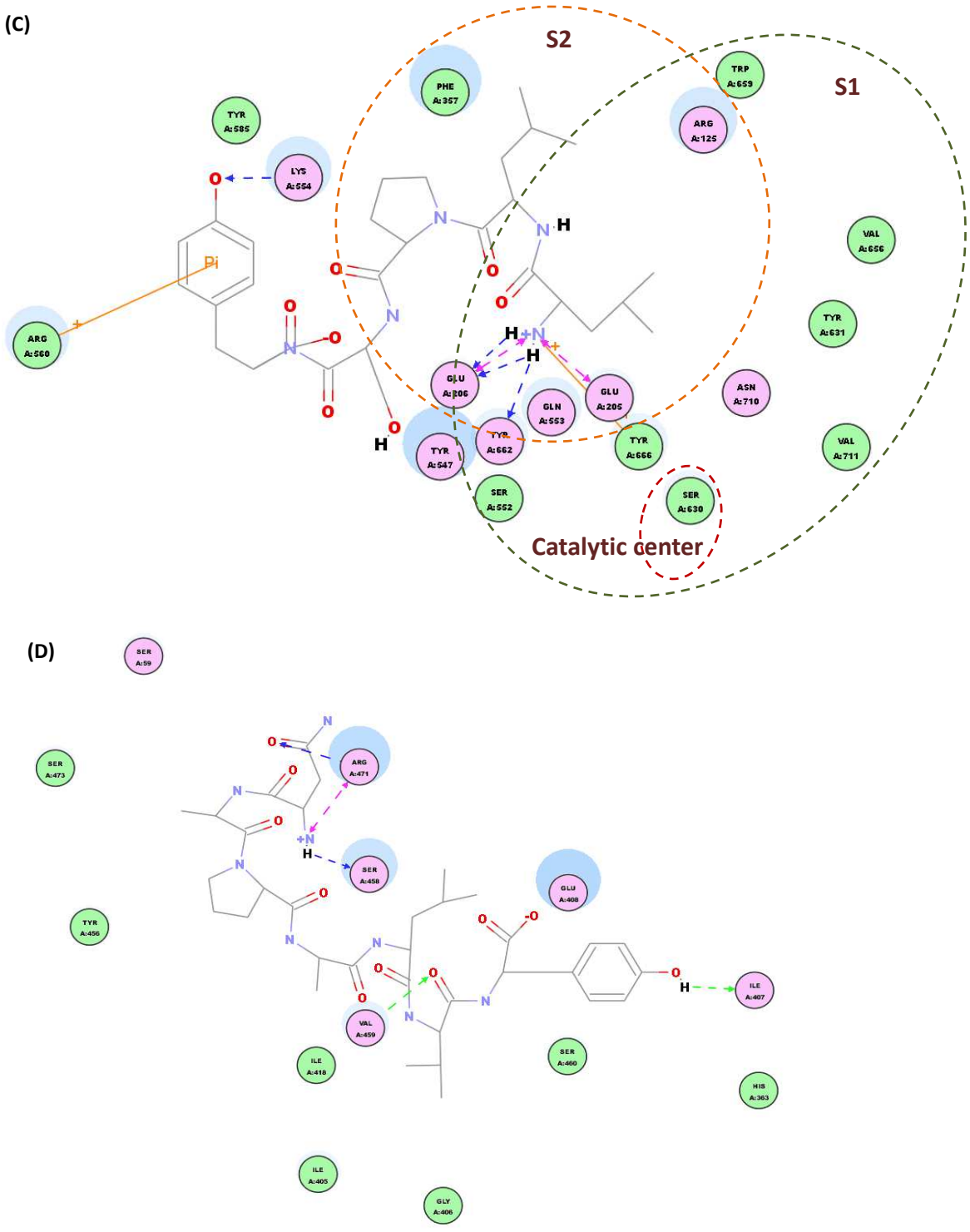


Figure 7. Molecular dicking simulation of the interaction of LY-5 and NY-7 against with ACE and DPP-IV. Best docking poses of (A) LY-5 and (B) NY-7 at the ACE receptor (PDB code: 1O86); (C) LY-5, (D) NY-7 at the DPP-IV receptor (PBD code: 1WCY). The dash circles indicate the amino residues in the active pockets.

Supplementary Files

This is a list of supplementary files associated with this preprint. Click to download.

- 20240312manuscriptSupMedicincalChemistryresearch.pdf